

Solvation of the Fluoride Anion by Methanol[†]

Charlotte A. Corbett, Todd J. Martínez, and James M. Lisy*

Department of Chemistry, University of Illinois at Urbana-Champaign, Urbana, Illinois 61801

Received: April 3, 2002; In Final Form: June 13, 2002

Solvation of the fluoride anion by methanol was investigated through vibrational predissociation spectroscopy of small cluster ions. The strong hydrogen-bond interaction between the anion and the hydroxyl group of methanol led to a shift of some O–H stretching frequencies into the C–H stretch region. The use of deuterated methanol (d_1 and d_3) was essential in isolating and identifying the C–H and O–H stretching modes. Ab initio calculations were used to determine infrared frequencies/intensities and optimized geometries. When the theoretical results were combined with the experimental observations, the fluoride anion was found to exhibit surface solvation. Evidence for methanol–methanol hydrogen-bond interactions appears when the fluoride anion is solvated by four or more methanol molecules. These results are consistent with previous studies, which show surface hydration of the chloride, bromide, and iodide anions and solvation of the chloride and iodide anions with methanol. However, these results contrast with the hydration of the fluoride anion, where the ion was found to undergo interior solvation with up to five water molecules.

I. Introduction

The study of clusters as a model for microscopic solvation can be useful in elucidating the nature of macroscopic properties. In ion clusters, solvation structures fall into two basic categories: interior and surface. Interior solvation occurs when the ion is at or near the center of mass of the cluster, leading to a quasi-symmetric structure. In surface solvation, the structure is asymmetric, with the solvent molecules aggregating to one side of the ion.

In solvents that are capable of hydrogen bonding, there is an inherent competition between ion–solvent and solvent–solvent interactions. For anions, this is most acute, because the ionic hydrogen bond between the ion and the solvent directly competes with the ability of the solvent to hydrogen bond with itself. As a result, there has been considerable interest in studying these systems from both experimental and theoretical perspectives. For the halide anions, which are arguably the simplest class of anions, the hydrated structures of chloride, bromide, and iodide are all surface-solvated.^{1,2} However, the fluoride anion was observed to be interior-solvated with three to five water molecules.³ Because of concerns that the cluster ion structures might depend on the amount of internal energy contained within the cluster, methods have been developed to study hydrated ions that are simultaneously solvated with argon,⁴ leading to significant cooling. Infrared spectra of cold clusters of $X^-(H_2O)_2$, where $X^- = F^-, Cl^-, Br^-,$ or I^- , have been obtained using this method and have indicated that water–water H-bonding occurs with Cl^- , Br^- , and I^- but not with F^- .⁵ These findings have been confirmed by recent ab initio calculations, where particular attention has been paid to the trends as a function of anion and as a function of size.^{6,7}

In warmer clusters, water–water H-bonding was observed in $Cl^-(H_2O)_{4,5}$ clusters.² Although no water–water H-bonding was observed for the smaller $Cl^-(H_2O)_{2,3}$ clusters, the water molecules appeared to be localized on one side of the ion and

not uniformly distributed about the ion.² A comparison with the hydration of F^- offers an interesting contrast by varying the solute ion. Ab initio calculations of $F^-(H_2O)_{4-6}$ clusters at 0 K indicated that only the pentahydrated ion was internally solvated, but at 298 K, all clusters exhibited internal solvation.⁸ This suggests that considerations of internal energy in experimental studies should be included in the characterization of cluster structures. In a combined experimental and theoretical investigation, it was concluded that $F^-(H_2O)_{3-5}$ clusters were interior-solvated from mass-selective infrared laser spectroscopy.³ In addition, water–water H-bonding was not observed, consistent with supporting ab initio calculations.³

The nature of anion hydration discussed above demonstrates a distinct difference between F^- and the other halides. This raises some interesting questions. Will similar differences occur with a different hydrogen-bonding solvent? This question, in turn, leads to the issue of whether this behavior strictly a property of the ion or whether the solvent also has a role in determining the nature of solvation. A similar solvent that would offer a meaningful comparison is methanol. In contrast to water, methanol has more limited hydrogen bonding, because of its single O–H group. Thus, a choice must be made between proton donation to an ion or to another methanol molecule; it cannot do both. In a previous study,⁹ Cl^- was determined to be surface-solvated in methanol. The onset for methanol–methanol H-bonding occurred with four methanol molecules, whereas the first shell for Cl^- in the condensed phase has nominally four to six molecules about the anion.¹⁰ A more recent investigation of Cl^- solvation in methanol favors the smaller value (approximately four in $LiCl$ and about two in $NiCl_2$ because of inner-shell complexing to Ni^{2+}).¹¹ Supporting ab initio calculations for a 3 + 1 asymmetric configuration (three molecules in the first shell and one in the second solvation shell) agreed with the experimental data.⁹ The nature of the solvation of Cl^- by water and methanol is the same, indicating that the nature of the ion might be responsible for the asymmetric solvation. It has been suggested that the large polarizability of the chloride

[†] Part of the special issue "Jack Beauchamp Festschrift".

* Corresponding author. E-mail: j-lisy@uiuc.edu.

anion leads to an asymmetric distribution of solvent about the anion.^{9,12–14}

By using F^- as the anion with methanol, a comparison of ion type can be made to the previous work. Vibrational spectra can be used to determine the onset of methanol–methanol H-bonding, and ab initio calculations can aid in the interpretation of the experimental spectra. Whereas F^- was interior-solvated by water, this evidence will determine the nature of F^- solvation by methanol. A recent report by Johnson and co-workers¹⁵ on $I^-(CH_3OH)_2$ indicates that two structural isomers are present. A 2 + 0 cluster with both methanols in the first shell and a 1 + 1 cluster with methanol–methanol hydrogen bonding of one methanol in the second solvent shell are observed in argon-cooled complexes.¹⁵ The observation of asymmetric solvation in this situation is not overly surprising, as the interaction between I^- and methanol results in the weakest anionic hydrogen bond for any of the halide anions.

Methanol is known to form strong hydrogen bonds with fluoride anion.¹⁶ This interaction leads to a large red shift in the OH stretching frequency (from 3681 cm^{-1} for the gas-phase methanol monomer¹⁷) when the anionic hydrogen bond is formed. This is commonly denoted as the O–H₁ stretch, i.e., the O–H stretch affected by the ionic H-bond with the anion. In the larger halides, the O–H₁ stretches were observed at 3241 cm^{-1} for the $Cl^-(CH_3OH)_2$ complex⁹ and at 3369 cm^{-1} for the $I^-(CH_3OH)_2$ species¹⁵ in which both molecules are bound to the anion. From data on hydrated fluoride clusters ions, where the O–H₁ frequency in $F^-(H_2O)_2$ is 2520 cm^{-1} ¹⁸ and that in $F^-(H_2O)_3$ is 2890 cm^{-1} ,³ one expects shifts of 800–1000 cm^{-1} for the methanol O–H₁ stretches in small $F^-(CH_3OH)_n$ clusters. Because the symmetric and two asymmetric C–H stretches of gas-phase methanol are 2844, 2970, and 2999 cm^{-1} , respectively,¹⁷ the O–H₁ band will likely overlap (and possibly interact) with the C–H stretches. As a result, infrared spectra using deuterated (d₁ and d₃) methanol were collected to decouple the O–H and C–H modes.

II. Experimental and Theoretical Methods

The method used to collect the vibrational predissociation spectra has been described previously,^{9,19,20} but a short account follows that highlights improvements made for this study. Fluoride anions generated by a thermionic emitter collide with methanol clusters produced by a molecular beam expansion, thus forming nascent $F^-(CH_3OH)_n$ clusters. These “hot” clusters stabilize by evaporative cooling^{21–23} and are analyzed by a tandem quadrupole mass spectrometer. A tunable infrared (IR) laser is used for vibrational excitation of the cluster ion of interest (selected by the first quadrupole), leading to the loss of a methanol molecule (via vibrational predissociation), resulting in an increase in the number of the $F^-(CH_3OH)_{n-1}$ fragment ions, which are contained by the second ion-guiding quadrupole and subsequently detected by the third quadrupole. The IR source is a Nd:YAG pumped optical parametric oscillator (OPO) laser with typical energies of 1–3 mJ/pulse and a tuning range of 2600–4000 cm^{-1} . The Nd:YAG pump laser is a custom Continuum Shure-lite instrument with the following operating parameters: 150 mJ/pulse (400 mJ/pulse maximum), 20-Hz repetition rate, and 19-ns pulse width. Absolute frequency calibration was performed simultaneously with the infrared spectra by collecting an absorbance spectrum of HCl between 2600 and 3100 cm^{-1} and an atmospheric water photoacoustic spectrum between 3350 and 3800 cm^{-1} . The peak frequencies in the vibrational spectra were assigned following fits to Lorentzian line shapes, which more closely fit the spectra than Gaussian line shapes.

Ab initio methods were used to determine both geometries and vibrational frequencies of $F^-(CH_3OH)_{1-4}$ clusters. The calculations performed were similar to those done previously for $Cl^-(CH_3OH)_n$.⁹ In this approach, the MP2-minimized geometry was found using a cc-pVDZ²⁴ basis set with diffuse functions on the fluoride, oxygen, and hydroxyl hydrogen atoms.²⁵ As discussed and justified in a previous paper,⁹ the vibrational frequencies were calculated at the HF level using the MP2-optimized geometry. The ab initio frequencies were adjusted by a scaling factor, determined from the ratio of the experimental¹⁷ to the calculated methanol monomer frequency, and are shown in Table 1. The ab initio stick spectra of frequencies and intensities were convoluted into Lorentzian line shapes with widths that best fit the experimental spectra.

III. Results and Discussion

A. $F^-(CH_3OH)_{3,4}$. Three distinct features are observed in the experimental spectrum of $F^-(CH_3OH)_3$ displayed in Figure 1, two relatively narrow bands near 2770 and 2855 cm^{-1} due to the symmetric and asymmetric C–H stretches and a broad feature centered near 3075 cm^{-1} from the O–H₁ stretch. These assignments are based on the theoretical frequencies from the ab initio calculations, which place all three molecules in the first solvent shell, hydrogen bonded to the F^- . The over 700 cm^{-1} shift of the O–H stretch is comparable to that observed in $F^-(H_2O)_3$.³ It is clear that the large shift in the methanol O–H₁ stretch results in an overlap with the C–H stretches. There is no indication of methanol–methanol H-bonding, which would be reflected by more than one O–H vibrational feature, although it is possible that overlap and/or the broad band could interfere with such observations. However, judging from the very good agreement with the theoretical frequencies, the spectrum of $F^-(CH_3OH)_3$ is consistent with the 3 + 0 structure, where all three molecules are in the first solvent shell.

The computed optimized geometry of the $F^-(CH_3OH)_3$ cluster has the methanol molecules on one side as depicted in Figure 1. This result is contrary to the structure of the $F^-(H_2O)_3$ cluster, where the molecules are equally spaced about the ion and the F and O atoms are coplanar.³ F^- was found to be internally solvated by water,³ so the above observation suggests that F^- might be surface-solvated by methanol.

As the number of molecules increases, so does the spectral complexity. Deuterated (d₃) methanol (vibrational frequencies have been determined by Bertie and co-workers²⁶) was used to simplify the $n = 4$ spectrum by eliminating the C–H stretches. Thus, only the O–H stretches remain in the 2700–3600 cm^{-1} region. The spectrum of $F^-(CD_3OH)_4$ is shown in Figure 2, where four distinct peaks are observed. One narrow band is observed at 2879 cm^{-1} . What appears to be a triplet (a prominent peak with two smaller peaks on either side) is observed near 3190 cm^{-1} . The band at 2879 cm^{-1} is at lower frequency than the O–H₁ peak for $F^-(CD_3OH)_3$ at 3074 cm^{-1} , indicating a stronger hydrogen bond than is present in $F^-(CH_3OH)_3$. This would be inconsistent with the strength of the hydrogen bond in a 4 + 0 configuration for $F^-(CH_3OH)_4$. As was noted above in the case of $F^-(H_2O)_{2,3}$, there is a weakening of the ionic hydrogen bond as the first shell fills. This is reflected in the smaller red shift of the O–H₁ stretching frequency. Similar behavior was observed in $Cl^-(CH_3OH)_{1-3}$ for the O–H₁ stretch.⁹

A second type of structure, a 3 + 1 configuration for $F^-(CD_3OH)_4$, might exist where three molecules are in the first solvent shell and one is in the second. Indeed, ab initio calculations indicate that the 3 + 1 and 4 + 0 structures have

TABLE 1: Summary of $F^-(CH_3OH)_n$, $n = 2-5$ Clusters^a

n	structure ^c	stretch ^d	experimental ^b			theoretical	
			frequency (cm ⁻¹)	width (cm ⁻¹)	area (10 ⁻¹⁸ cm)	frequency ^e (cm ⁻¹)	intensity ^f
3	2 + 1	O-H_{EI}				2337	65.5
	2 + 1	C-H_s				2786	21.7
	3 + 0	C-H _s	2769 ± 1	56 ± 3	29 ± 2	2801	13.2
	2 + 1	C-H_a				2907	20.9
	3 + 0	C-H _a	2854 ± 2	106 ± 8	44 ± 4	2921	23.4
	2 + 1	O-H_I				2937	7.0
	3 + 0	O-H _I	3074 ± 10	388 ± 26	69 ± 5	3044	55.8
	2 + 1	O-H_T				3167	24.9
4	3 + 1	O-H_{EI}	2879 ± 1	60 ± 5	57 ± 9	2768	56.1
	3 + 1	C-H_s				2812	13.4
	4 + 0	C-H _s	2802 ± 1	32 ± 3	20 ± 3	2813	10.2
	3 + 1	C-H_a				2928	23.0
	4 + 0	C-H _a	2934 ± 8	106 ± 21	38 ± 13	2930	21.4
	3 + 1	O-H_I	3084 ± 3	112 ± 16	38 ± 8	3070	43.5
	4 + 0	O-H _I	3190 ± 2	95 ± 9	54 ± 7	3180	90.4
	3 + 1	O-H_T	3299 ± 4	136 ± 11	49 ± 5	3300	21.7
5	5 + 0, 4 + 1	C-H _s	2808 ± 1	41 ± 3	45 ± 4		
	5 + 0, 4 + 1	C-H_a	2901 ± 2	113 ± 7	117 ± 7		
	4 + 1	O-H_{EI}	3090 ± 4	94 ± 14	38 ± 5		
	5 + 0	O-H _I	3233 ± 1	74 ± 4	95 ± 6		
	4 + 1	O-H_T	3350 ± 2	108 ± 7	93 ± 5		

^a Experimental values determined from Lorentzian fits of the spectra. ^b Entries for experimental results are made consistent with experimental data. ^c $n_1 + n_2$ indicates a structure with n_1 molecules in the first shell and n_2 molecules in the second shell. All properties for structures with $n_2 = 1$ (H-bonding) are highlighted in bold for clarity. ^d O-H_I indicates ionic hydrogen bond, O-H_{EI} indicates an enhanced O-H_I, and O-H_T indicates a terminal O-H stretch. C-H_s indicates a symmetric C-H stretch, and C-H_a indicates an asymmetric C-H stretch. ^e Theoretical frequencies were adjusted by a scaling factor determined from the ratio of the experimental (ref 12) to the ab initio methanol monomer frequency. The scaling factors for the C-H_s, C-H_a, and O-H stretches are 0.923, 0.941, and 0.954, respectively. An average scaling factor was used in instances when two different types of bands overlapped. ^f Theoretical intensity is in units of D²/amu·Å².

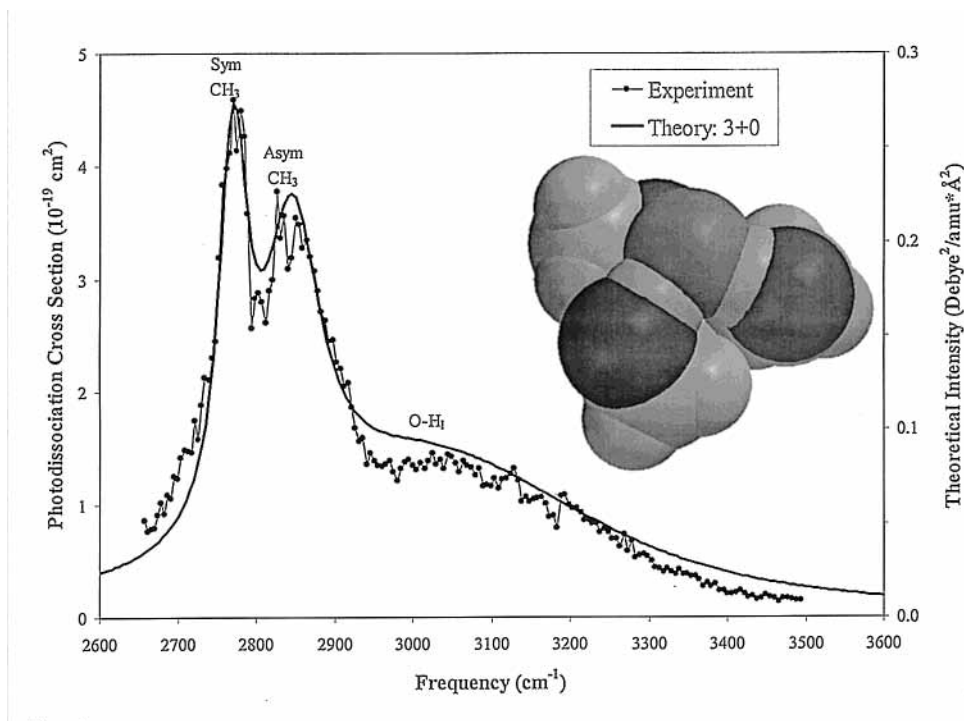


Figure 1. Vibrational spectrum and convoluted ab initio stick spectrum with Lorentzian line shapes of $F^-(CH_3OH)_3$. Graphical representation of $F^-(CH_3OH)_3$ using the optimized geometry from the ab initio calculation. The ab initio symmetric and asymmetric C-H stretch frequencies are shifted by -30 and -75 cm⁻¹, respectively. The full widths at half-maximum for the symmetric C-H, asymmetric C-H, and O-H_I stretches are 40, 90, and 400 cm⁻¹, respectively.

comparable energies (vide infra). As was observed in $I^-(CH_3OH)_2$ and $Cl^-(CH_3OH)_4$, the O-H stretching frequency of the first-shell methanol, which acts as the proton acceptor of the second-shell methanol, gains an additional significant shift to lower frequency. The ionic hydrogen bond in this first-shell

methanol is cooperatively *enhanced* by accepting the hydrogen bond from the second-shell methanol. Denoting this type of O-H stretch as O-H_{EI}, the additional shift in frequency has been observed to be about 200 cm⁻¹ in $I^-(CH_3OH)_2$ ¹⁵ and $Cl^-(CH_3OH)_4$.⁹ Although one might anticipate a stronger

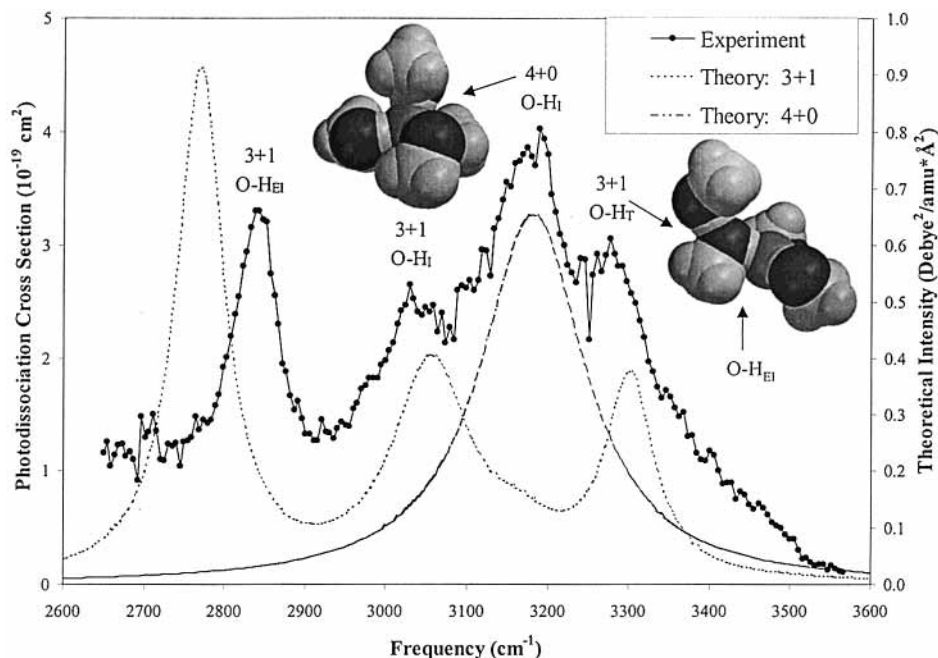


Figure 2. Vibrational spectrum of $F^-(CD_3OH)_4$ and convoluted ab initio stick spectra with Lorentzian line shapes of the 3 + 1 and 4 + 0 structural isomers of $F^-(CH_3OH)_4$ O-H frequencies. The full widths at half-maximum for the O-H_{EI}, O-H_I, and O-H_T stretches of the 3 + 1 structure and the O-H_I stretch of the 4 + 0 structure are 125, 200, 125, and 275 cm^{-1} , respectively. Graphical representations of the 4 + 0 and 3 + 1 structures of $F^-(CH_3OH)_4$ using the optimized geometries from the ab initio calculations are also provided.

enhancement in the case of Cl^- , the O-H_I stretches for $I^-(CH_3OH)_1$ and $Cl^-(CH_3OH)_3$ were observed at 3331 and 3325 cm^{-1} , respectively,^{9,15} suggesting comparable anionic hydrogen-bond strengths. A 3 + 1 configuration should have an O-H_{EI} stretch to lower frequency than the O-H_I stretch of a 3 + 0 structure—an assumption that is confirmed by ab initio calculations (see Table 1) and by comparison with $Cl^-(CH_3OH)_{3,4}$.⁹ Thus, the band at 2879 cm^{-1} can be assigned to an O-H_{EI} stretch of a 3 + 1 structure. Again, this band is shifted by about 200 cm^{-1} to lower frequency than the O-H_I band in $F^-(CH_3OH)_3$, which is consistent with the shifts observed in $I^-(CH_3OH)_2$ ¹⁵ and $Cl^-(CH_3OH)_4$.⁹ There are two other first-shell methanol molecules in $F^-(CD_3OH)_4$ with O-H_I bands that can be expected to be in the same frequency region as the O-H_I band in $F^-(CH_3OH)_3$ (3074 cm^{-1} , see Table 1). The peak at 3084 cm^{-1} is assigned to the O-H_I stretches of the 3 + 1 structure, as indicated in Figure 2. The peak at highest frequency, 3300 cm^{-1} , is most likely from the terminal O-H, O-H_T, stretch (the O-H stretch of the second-shell methanol). These are the three O-H stretching bands associated with the 3 + 1 configuration. As can be seen in Figure 2, they are in good agreement with the frequencies obtained from the ab initio calculations. The remaining and prominent feature at 3190 cm^{-1} must be due to the 4 + 0 configuration. This structure would also have only a single infrared-active O-H stretching band, the O-H_I, which should be slightly higher in frequency than the 3 + 1 O-H_I band [and the O-H_I band in 3 + 0 $F^-(CH_3OH)_3$]. The results from the ab initio calculations again confirm this assignment of the infrared-active O-H_I stretch to within 10 cm^{-1} of the observed experimental value, as shown in Table 1. Which of the two configurations is most stable? The results from the calculation place the 4 + 0 configuration lower in energy by 2.7 kcal/mol, which narrows to 2.2 kcal/mol when zero-point energy (in the harmonic approximation) is taken into account. As these two configurations are so close in energy, it is no surprise that both are represented in the experimental observations, where the internal energy content

of $F^-(CD_3OH)_4$, as estimated by the evaporative ensemble,^{21–23} is equivalent to approximately 300 K.

The spectrum of $F^-(CH_3OH)_4$ is shown in Figure 3 for completeness. The ab initio frequencies are in good agreement with the experimental data. As can be observed, the overlap between the O-H_{EI} band in the 3 + 1 structure and the C-H stretching modes would have made structural assignments difficult in the absence of the CD_3OH measurements. The use of d_3 methanol was crucial to the interpretation and identification of the two $F^-(CH_3OH)_4$ structural isomers. In $F^-(H_2O)_n$ clusters, there was no indication of water–water H-bonding with up to five molecules.³ Because H-bonding between the methanol molecules begins prior to the filling of the first solvent shell, this is evidence that the $F^-(CH_3OH)_4$ cluster exhibits surface solvation. The presence of a 4 + 0 structure indicates a competition between surface and interior solvation at this cluster size.

In comparing Figure 1 with either Figure 2 or 3, it is clear that the breadth of the hydrogen-bonded OH stretch is much larger for the smaller $F^-(CH_3OH)_3$ cluster ion. There are two likely reasons. First, the smaller number of solvent molecules allows for greater motion within the first solvent shell, thus giving rise to a wide range of structural conformers. The clusters with four solvents have less mobility about the ion, resulting in a more defined first solvent shell. A second possibility is related to the effective temperature of the cluster ions. The solvent binding energies decrease with increasing solvent number in this size range.¹⁶ The internal energy or effective temperature of the cluster ions also decreases with increasing solvent number as expected from the evaporative ensemble.^{22,23} Cluster ions with greater internal energy will have more excitation in vibrational modes associated with the anionic hydrogen bond. This will modulate the distance between the anion and the methanol molecules, varying the strength of the ionic hydrogen bond and leading to a broadening of the O-H stretching band. The $F^-(CH_3OH)_3$ cluster ion with its higher internal energy would accordingly have a broader band than $F^-(CH_3OH)_4$.

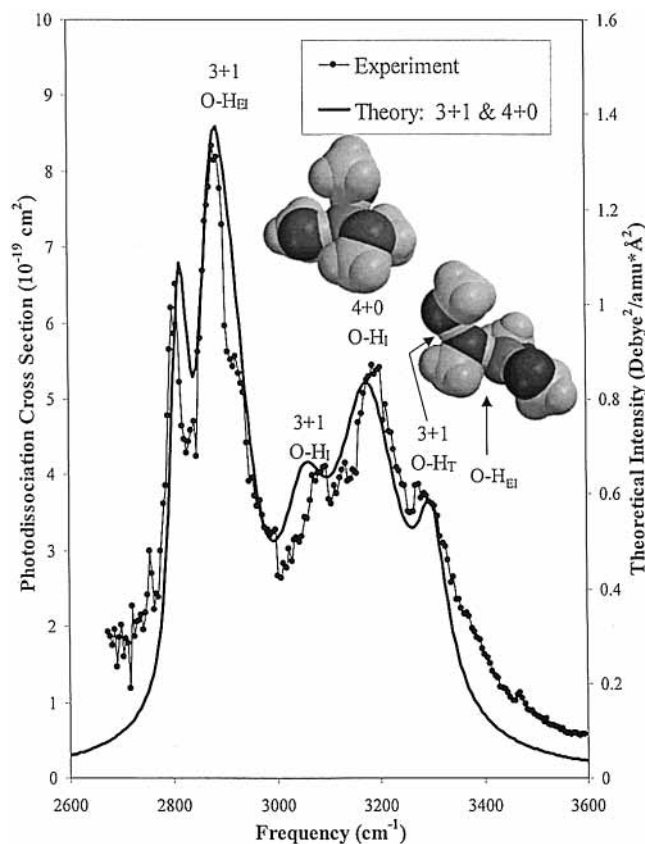


Figure 3. Vibrational spectrum of $F^-(CH_3OH)_4$ and summation of the 3 + 1 and 4 + 0 $F^-(CH_3OH)_4$ structural isomers convoluted ab initio stick spectrum with Lorentzian line shapes. The O–H_{EI} feature of the 3 + 1 structure is shifted by 110 cm^{-1} . The full width at half-maximum (fwhm) for the O–H_I feature of the 4 + 0 structure is 275 cm^{-1} . The fwhm values for the O–H_{EI}, O–H_I, and O–H_T features of the 3 + 1 structure are 138, 200, and 125 cm^{-1} , respectively. Graphical representations of the 4 + 0 and 3 + 1 structures of $F^-(CH_3OH)_4$ using the optimized geometries from the ab initio calculations are also provided.

B. $F^-(CH_3OH)_{5-8,10,12,13}$. From the observations on the smaller $F^-(CH_3OH)_{3,4}$ cluster ions and previous studies on $I^-(CH_3OH)_{1,2}$ ¹⁵ and $Cl^-(CH_3OH)_n$,⁹ the shift to lower frequency of the O–H_I band from the gas-phase monomer value decreases as the number of methanol molecules increases (note that the computed frequencies for the O–H_I stretches of $F^-(CH_3OH)_{1,2}$ are 2089 and 2720 cm^{-1} , respectively). This trend continues for the larger $F^-(CH_3OH)_n$ cluster ions as well. This is due to a weakening of the electrostatic interaction/binding energy, and thus the anionic hydrogen-bond strength, as the cluster size increases. In a qualitative sense, the shift drops off rapidly with decreasing binding energy.²⁷ From extrapolation, the O–H_I frequency for the 5 + 0 cluster should be about 3240 cm^{-1} , in the middle of the 120 cm^{-1} span between the 4 + 0 O–H_I and 3 + 1 O–H_T stretching frequencies. The most prominent peak in the $F^-(CH_3OH)_5$ spectrum occurs at 3233 cm^{-1} , as shown in Figure 4. This could be attributed to the O–H_I stretch in a 5 + 0 configuration, although a 4 + 1 O–H_I is also a possibility. Because the peak is so prominent and is part of a “triplet”, it seems unlikely that only one configuration for $F^-(CH_3OH)_5$ is present. The features on either side of the peak at 3233 cm^{-1} follow from the designations given for $n = 4$. For clusters with five or more methanol molecules, we were unable to do ab initio calculations of sufficient quality to address the O–H stretching frequency issues quantitatively. Thus the remaining assignments are based on the trends observed for the smaller cluster ions.

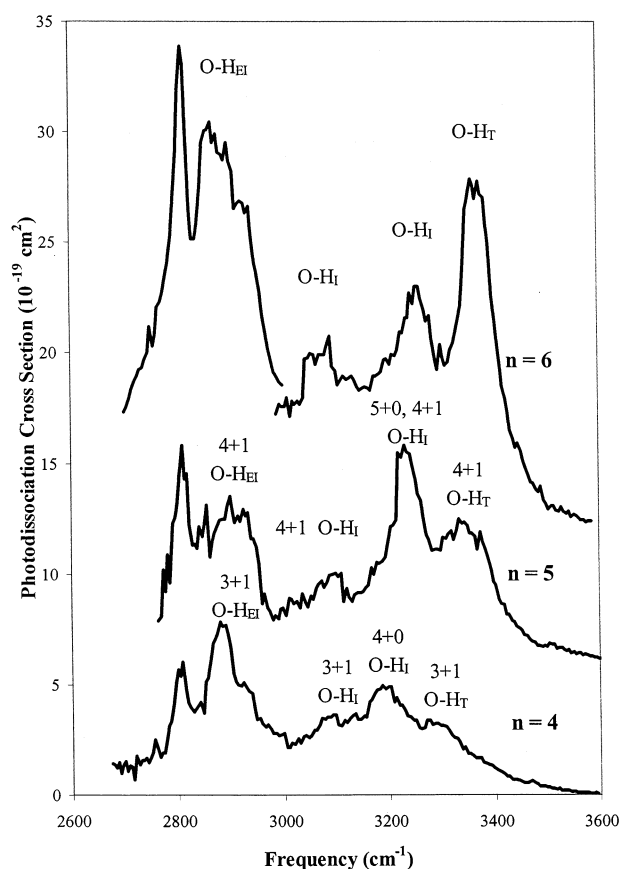


Figure 4. Vibrational spectra of $F^-(CH_3OH)_n$, $n = 4-6$. The spectra of $n = 5$ and 6 are offset by 6 and 12 $\times 10^{-19} cm^2$, respectively. The O–H_{EI} bands heavily overlap with the methyl CH_3 symmetric and asymmetric stretches.

The highest-frequency peak in all of the large cluster ion spectra is expected to be from the O–H_T stretch. This vibrational mode is not as dependent on the ion and should always be less than or about equal to the O–H_T stretching frequency of linear methanol trimer,^{28,29} 3433 cm^{-1} . Note that, in $I^-(CH_3OH)_2$, the O–H_T frequency in the 1 + 1 cluster ion was 3340 cm^{-1} , whereas in $Cl^-(CH_3OH)_{4-12}$ cluster ions, these bands were observed between 3380 and 3465 cm^{-1} . The O–H_T stretching frequencies for the larger $F^-(CH_3OH)_{5-13}$ clusters are displayed in Table 2 and gradually increase with increasing cluster size, tending from 3350 to 3440 cm^{-1} . This common behavior, shared by the three methanolated anions and the neutral linear methanol trimer, lends considerable support to this assignment.

There are at least two possible structural isomers for $n = 5$, and similar numbers are believed to occur for $n = 6$. A 6 + 0 structure is unlikely, principally because of the high intensity of the O–H_T bands that dominate this region of the spectrum. From extrapolation of the O–H_I frequencies of the smaller clusters, the 6 + 0 O–H_I band should occur at 3270 cm^{-1} , where there is relatively little intensity. All peaks are assigned by comparison with the $n = 5$ spectrum. However, with the likelihood of many different structures and conformations, the assignment of specific configurations is somewhat speculative.

As the cluster size increases to seven, it becomes more difficult to separate, identify, and assign individual peaks between 3000 and 3300 cm^{-1} , the region mainly consisting of O–H_I features, as seen in the spectra shown in Figure 5. There are some general trends, and information can be gained from Lorentzian fits to the data, given in Table 2. At first, the O–H_T feature increases in intensity with cluster size, reflecting higher

TABLE 2: Summary of $F^-(CH_3OH)_n$, $n = 6-8, 10, 12, 13$, Clusters^a

n	stretch ^b	frequency (cm ⁻¹)	width (cm ⁻¹)	area (10 ⁻¹⁸ cm ²)
6	C-H _s	2809 ± 1	16 ± 3	24 ± 4
	C-H _a	2868 ± 2	211 ± 6	560 ± 13
	O-H _{EI}			
	O-H _{EI}	3094 ± 4	76 ± 16	45 ± 9
	O-H _I	3246 ± 3	119 ± 12	149 ± 14
	O-H _T	3372 ± 1	67 ± 4	151 ± 8
7	C-H _s	2815 ± 1	18 ± 1	30 ± 2
	C-H _a and O-H _{EI}	2894 ± 2	148 ± 6	225 ± 9
	O-H _I and O-H _{EI}	3114 ± 4	155 ± 16	131 ± 16
	O-H _I	3261 ± 3	126 ± 15	101 ± 14
	O-H _T	3394 ± 1	66 ± 2	130 ± 5
8	O-H _I and O-H _{EI}	3125 ± 2	175 ± 11	311 ± 20
	O-H _I	3274 ± 3	99 ± 12	89 ± 13
	O-H _T	3402 ± 1	63 ± 2	184 ± 5
10	O-H _I and O-H _{EI}	3154 ± 3	168 ± 17	265 ± 36
	O-H _I	3291 ± 3	120 ± 14	122 ± 19
	O-H _T	3424 ± 1	60 ± 2	125 ± 5
12	C-H _s	2851 ± 1	33 ± 3	82 ± 8
	C-H _a and O-H _{EI}	2933 ± 2	98 ± 8	213 ± 17
	O-H _I and O-H _{EI}	3141 ± 5	157 ± 22	218 ± 40
	O-H _I	3291 ± 3	156 ± 14	358 ± 41
	O-H _T	3440 ± 1	55 ± 4	139 ± 10
13	C-H _s	2826 ± 1	23 ± 3	43 ± 5
	C-H _a and O-H _{EI}	2922 ± 2	151 ± 11	273 ± 20
	O-H _I and O-H _{EI}	3227 ± 4	297 ± 19	459 ± 28
	O-H _T	3439 ± 3	63 ± 13	41 ± 9

^a Values determined from Lorentzian fits of the experimental spectra.

^b O-H_I is an O-H stretch involved in an ionic hydrogen bond, and O-H_{EI} is an enhanced O-H_I, where the molecule is also acting as a proton acceptor to another methanol molecule. C-H_s indicates a symmetric methyl stretch, and C-H_a indicates an asymmetric methyl stretch.

occupancy in the second solvent shell. Whereas the intensity, given by the area of the band, maximizes at $n = 8$, the maximum ratio of the O-H_T peak area to the O-H_I region occurs at $n = 6$. This indicates that structures with significant numbers of second-shell methanols are present. As the cluster size increases further, the intensity in the region between 3000 and 3300 cm⁻¹ becomes dominant. The O-H stretch for liquid methanol is at 3351 cm⁻¹, so this region would be expected to increase in intensity as methanol-methanol H-bonding becomes more extensive. At $n = 13$, there is no longer much distinction between different O-H stretches, as one very broad band around 3230 cm⁻¹ begins to consolidate. The degradation of distinct spectral features suggests an amorphous structure with the cluster resembling a microscopic solution.

C. $F^-(CH_3OD)_{2-8}$. Whereas the O-H group has been used to monitor the strength of the interaction between the halide anion and methanol, it is also possible to examine the effects on the CH₃ portion of the molecule. Figure 6 contains spectra of $F^-(CH_3OD)_n$, $n = 2-8$. The use of the d₁ isotopomer²⁶ eliminates spectral congestion from the O-H_{EI} bands that would otherwise occur in the same region.

The spectra of $n = 2$ and 3 are relatively broad and diffuse, whereas the bands for $n = 4$ are narrower and more defined, as exemplified in Table 3. The binding energies for $F^-(CH_3OH)_3$, $Cl^-(CH_3OH)_2$, and $Na^+(CH_3OH)_4$ are similar, so their internal energies should be similar in our apparatus. The temperatures of $Cl^-(CH_3OH)_2$ and $Na^+(CH_3OH)_4$ were determined to be about 380 and 340 K, respectively.^{9,30} The effective barrier to internal rotation for methanol monomer is 370 cm⁻¹, or 540 K.³¹ In methanol dimer, the barrier to internal rotation for the

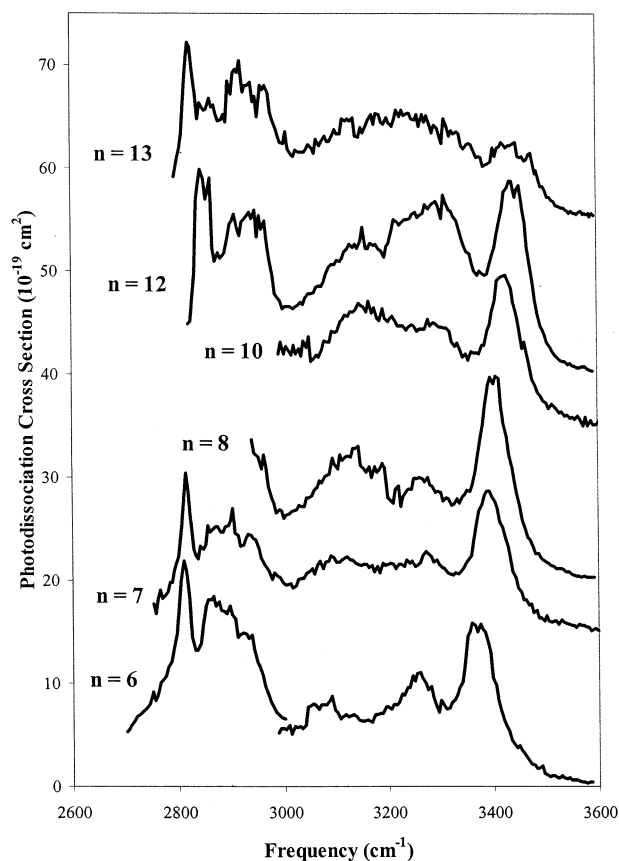


Figure 5. Vibrational spectra of $F^-(CH_3OH)_n$, $n = 6-8, 10, 12, 13$. The spectra of $n = 7, 8, 10, 12$, and 13 are offset by 15, 20, 35, 40, and 55 × 10⁻¹⁹ cm², respectively.

proton donor decreases to 265 K for the donor methyl group.³¹ Because all methanol molecules in $F^-(CH_3OH)_n$ clusters act as proton donors, it is expected that the barrier will be comparable if not lower in these clusters. Thus, it is likely that there is sufficient internal energy for $F^-(CH_3OH)_{2,3}$ to overcome the barrier for internal rotation, leading to the broad C-H bands. As the clusters increase in size, the internal energy will drop to the limiting value, determined by the methanol-methanol binding energy of ~170–200 K.³⁰ The clusters no longer have sufficient energy to overcome the internal rotation barrier, resulting in sharper and more structured bands. It is interesting to observe that the behavior of the width of the C-H stretching bands is opposite to that of the O-H stretching modes.

The other noticeable trend observed with increasing cluster size is the convergence of the bands toward the frequencies of the C-H stretches in liquid-phase CH₃OD. These values are shown in Figure 5. Here, the C-H stretches begin to emulate liquidlike behavior just as the O-H stretches outlined in the preceding section did.

IV. Conclusions

Solvation of the fluoride anion by methanol has been explored. It should be noted that, in this analysis, spectra with deuterated methanol were essential for band identification because of the overlap of C-H bands with ionic hydrogen-bonded O-H stretching modes. The O-H_I and O-H_{EI} frequencies are seen to increase with increasing cluster size, whereas the O-H_T stretching frequency displays a less dramatic variation. The onset of methanol-methanol H-bonding occurs with four methanol molecules. Extensive methanol-methanol H-bonding tends to dominate specific O-H stretches at a cluster

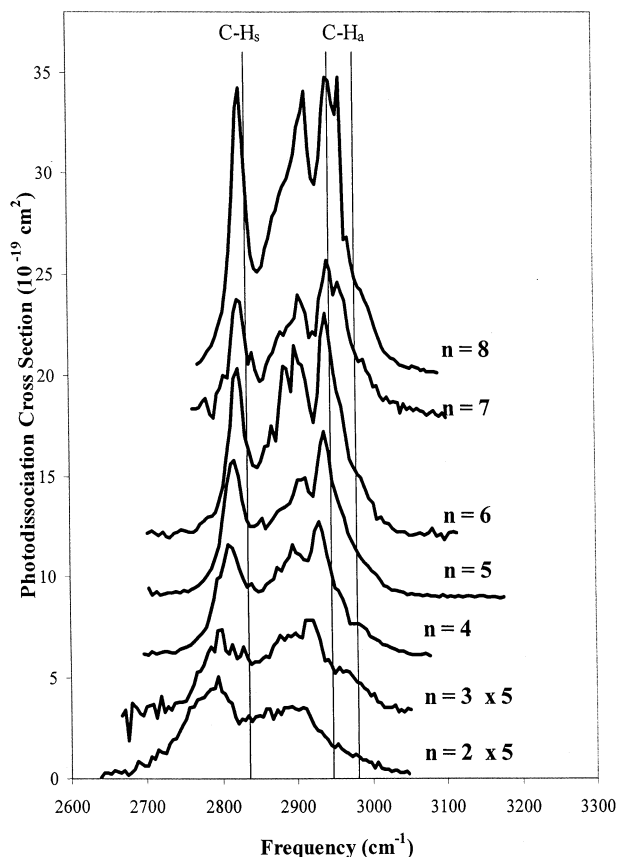


Figure 6. Vibrational spectra of $F^-(CH_3OD)_n$, $n = 2-8$. The vertical lines represent the frequencies of the symmetric and asymmetric C-H stretches of liquid CH_3OD , the values of which are from ref 26. The spectra of $n = 2$ and 3 are scaled by a factor of 5. The spectra of $n = 3-8$ are offset by 3, 6, 9, 12, 18, and $20 \times 10^{-19} \text{ cm}^2$, respectively.

TABLE 3: Summary of $F^-(CH_3OD)_n$, $n = 2-8$, Clusters^a

n	symmetric C-H		asymmetric C-H			
	frequency	width	frequency	width	frequency	width
2	2784 ± 1	78 ± 3	2892 ± 2	103 ± 5		
3	2798 ± 2	55 ± 6	2906 ± 2	107 ± 6		
4	2811 ± 1	39 ± 3	2888 ± 3	80 ± 10	2934 ± 1	41 ± 5
5	2817 ± 1	28 ± 2	2891 ± 3	79 ± 11	2941 ± 1	43 ± 4
6	2822 ± 1	22 ± 2	2894 ± 1	55 ± 5	2946 ± 1	38 ± 3
7	2825 ± 1	21 ± 2	2897 ± 2	55 ± 8	2953 ± 1	50 ± 4
8	2827 ± 1	19 ± 2	2904 ± 2	69 ± 7	2953 ± 1	34 ± 4

^a Values, in cm^{-1} , determined from Lorentzian fits of the experimental spectra.

size of 13. The optimized geometries, from ab initio calculations, suggest that the methanol molecules aggregate to one side of the ion for the smaller clusters. The nature of the solvent does appear to play a role in the type of ion solvation. Methanol favors surface solvation for all halide anions, whereas the fluoride anion is interior-solvated by water.³ The C-H stretching modes exhibit a more subtle variation with cluster size. The smaller and warmer clusters appear to undergo free internal rotation.

Acknowledgment. This material is based on work supported in part by the National Science Foundation under Grants CHE-0072178 (to J.M.L.) and CHE-9733403 (to T.J.M.). We thank Mr. Sean M. Foradori for his assistance with the ab initio calculations of the $F^-(CH_3OH)_{1-4}$ cluster ions. One of the authors (J.M.L.) expresses his gratitude to Jack Beauchamp for his many contributions to the field.

References and Notes

- (1) Ayotte, P.; Weddle, G. H.; Johnson, M. A. *J. Chem. Phys.* **1999**, *110*, 7129-7132.
- (2) Choi, J.-H.; Kuwata, K. T.; Cao, Y.-B.; Okumura, M. *J. Phys. Chem.* **1998**, *102*, 503-507.
- (3) Cabarcos, O. M.; Weinheimer, C. J.; Lisy, J. M.; Xantheas, S. S. *J. Chem. Phys.* **1999**, *110*, 5-8.
- (4) Ayotte, P.; Weddle, G. H.; Kim, J.; Johnson, M. A. *Chem. Phys.* **1998**, *239*, 485-491.
- (5) Ayotte, P.; Nielsen, S. B.; Weddle, G. H.; Johnson, M. A.; Xantheas, S. S. *J. Phys. Chem.* **1999**, *103*, 10665-10669.
- (6) Kim, J.; Lee, H. M.; Suh, S. B.; Majumdar, D.; Kim, K. S. *J. Chem. Phys.* **2000**, *113*, 5259-5272.
- (7) Lee, H. M.; Kim, D.; Kim, K. S. *J. Chem. Phys.* **2002**, *116*, 5509-5520.
- (8) Baik, J.; Kim, J.; Majumdar, D.; Kim, K. S. *J. Chem. Phys.* **1999**, *110*, 9116-9127.
- (9) Cabarcos, O. M.; Weinheimer, C. J.; Martinez, T. J.; Lisy, J. M. *J. Chem. Phys.* **1999**, *110*, 9516-9526.
- (10) Yamagami, M.; Wakita, H.; Yamaguchi, T. *J. Chem. Phys.* **1995**, *103*, 8174-8178.
- (11) Adya, A. K.; Kalugin, O. N. *J. Chem. Phys.* **2000**, *113*, 4740-4750.
- (12) Dang, L. X.; Smith, D. E. *J. Chem. Phys.* **1993**, *99*, 6950-6956.
- (13) Knipping, E. M.; Lakin, M. J.; Foster, K. L.; Jungwirth, P.; Tobias, D. J.; Gerber, R. B.; Dabdub, D.; Finlayson-Pitts, B. J. *Science* **2000**, *288*, 301-306.
- (14) Jungwirth, P.; Tobias, D. J. *J. Phys. Chem. A* **2002**, *106*, 379-383.
- (15) Robertson, W. H.; Karapetian, K.; Ayotte, P.; Jordan, K. D.; Johnson, M. A. *J. Chem. Phys.* **2002**, *116*, 4853-4857.
- (16) Hiraoka, K.; Yamabe, S. *Int. J. Mass Spectrom. Ion Processes* **1991**, *109*, 133-150.
- (17) Serrallach, A.; Meyer, R.; Gunthard, H. H. *J. Mol. Spectrosc.* **1974**, *52*, 94-129.
- (18) Ayotte, P.; Nielsen, S. B.; Weddle, G. H.; Johnson, M. A.; Xantheas, S. S. *J. Phys. Chem. A* **1999**, *103*, 10665-10669.
- (19) Weinheimer, C. J.; Lisy, J. M. *J. Chem. Phys.* **1996**, *105*, 2938-2941.
- (20) Weinheimer, C. J.; Lisy, J. M. *Chem. Phys.* **1998**, *239*, 357-368.
- (21) Cabarcos, O. M.; Weinheimer, C. J.; Lisy, J. M. *J. Phys. Chem. A* **1999**, *103*, 8777-8791.
- (22) Klots, C. E. *J. Chem. Phys.* **1985**, *83*, 5854-5860.
- (23) Klots, C. E. *Z. Phys. D* **1987**, *5*, 83-89.
- (24) Dunning, T. H., Jr. *J. Chem. Phys.* **1989**, *90*, 1007-1023.
- (25) Kendall, R. A.; Dunning, T. H., Jr.; Harrison, R. J. *J. Chem. Phys.* **1992**, *96*, 6796-6806.
- (26) Bertie, J. E.; Zhang, S. L. *J. Mol. Struct.* **1997**, *413-414*, 333-363.
- (27) Miller, R. E. *Science* **1988**, *240*, 447-53.
- (28) Coussan, S.; Bakkas, N.; Loutellier, A.; Perchard, J. P.; Racine, S. *Chem. Phys. Lett.* **1994**, *217*, 123-130.
- (29) Zwier, T. S. *Annu. Rev. Phys. Chem.* **1996**, *47*, 205-241.
- (30) Cabarcos, O. M.; Weinheimer, C. J.; Lisy, J. M. *J. Phys. Chem. A* **1999**, *103*, 8777-91.
- (31) Lovas, F. J.; Hartwig, H. *J. Mol. Spectrosc.* **1997**, *185*, 98-109.